Spectroscopy of Hydrothermal Reactions. 6. Kinetics and Pathway of Conversion of Carbohydrazide to CO_2 and N_2H_4 at 503−543 K

J. W. Schoppelrei and T. B. Brill*

Department of Chemistry and Biochemistry, University of Delaware, Newark, Delaware 19716

Received: June 18, 1996; In Final Form: August 19, 1996[⊗]

Spectrokinetic analysis by IR spectroscopy was performed on 1.07 *m* carbohydrazide, $(NH_2NH)_2C{=}O$, in a Pt/Ir flow cell with diamond windows. The reaction rate at five temperatures between 503 and 543 K at 275 bar pressure was obtained. A lumped kinetic scheme involving two rate constants is proposed for the conversion of carbohydrazide to CO_2 and N_2H_4. In the first step carbohydrazide decays by pseudo-first-order kinetics ($E_a = 88 \pm 1$ kJ mol^{-1}, $\ln(A/s^{-1}) = 18$). $\Delta S^{\ddagger} = -108$ J mol^{-1} K^{-1}, which is consistent with the involvement of H_2O in the cleavage of the C−N bond. The main intermediate thus formed is proposed to be the hydrazinium salt of hydrazacarboxylate, which can exist in equilibrium forms. This intermediate decomposes in the second stage of the reaction to N_2H_4 and CO_2 with global Arrhenius parameters of $E_a = 57 \pm 1$ kJ mol^{-1} and $\ln(A/s^{-1}) = 10$ for the initial 10−15% of conversion to CO_2. At higher percentage of conversion, the rate of formation of CO_2 greatly accelerates, which suggests autocatalysis. The catalyst is proposed to be CO_2 by its effect on the hydrogen ion concentration.

Introduction

Owing to the fact that carbohydrazide, $(NH_2NH)_2C{=}O$, is a ready source of hydrazine when reacted with H_2O, it has application as a scavenger of O_2 in H_2O[1] and is especially noteworthy as a corrosion inhibitor in hot-water boilers used in power generation.[2,3] As such, the hydrothermolysis chemistry of aqueous carbohydrazide is important in practice, but the details appear not to have been investigated.

Although no previous kinetic measurements were found for aqueous carbohydrazide, the initial step of thermal decomposition of neat carbohydrazide has been described[4] to be the cyclization−elimination reaction in eq 1 which produces the five-membered tetrazolidine compound shown.

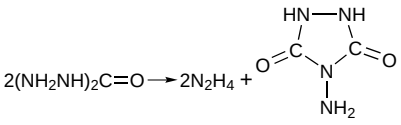

(1)

In aqueous solution, however, it is reasonable to anticipate that H_2O might participate in the reaction. Insertion of H_2O into the C−N bond could occur, leading ultimately to the products of eq 2. Intermediates, such as hydrazacarboxylic acid and its salts, which have been synthesized by other routes,[5] might be involved.

$$(NH_2NH)_2C{=}O + H_2O \rightarrow CO_2 + 2N_2H_4 \qquad (2)$$

In this article, the pathway and kinetics of the hydrothermolysis of aqueous carbohydrazide are proposed for the 503−543 K range under a pressure of 275 bar. These conditions are below the critical temperature (647 K) and above the critical pressure (221 bar) of pure H_2O. The resulting fluid density is 0.8−0.85 kg/dm^3 during the measurements. A Pt/Ir flow cell fitted with diamond wafer windows was used in conjunction with real-time FTIR spectroscopy during the reaction.[6,7] A description of the essential features of the reaction is obtained for the first time under hydrothermal conditions.

Experimental Section

We have recently described small-scale, high-precision flow cells[6,7] for IR spectroscopy which permit real-time, *in situ* interrogation of reactions in H_2O under extreme conditions. The reactions described herein were conducted and observed using the flow cell constructed of Pt/Ir alloy and Au fitted with type IIa diamond windows.[6] The pressure (±1 bar), temperature (±1 K), and flow rate (±0.01 mL/min, pulseless) remain well controlled The temperature was monitored in real time by a thermocouple mounted in the cell block in close proximity to the duct containing the windows. In previous work using the vapor−liquid phase boundary of pure H_2O,[6] it was determined that the absolute temperature is accurate to within ±1.5 K. The fluid temperature was assumed to be uniform despite the existence of laminar flow in the entrance regime. This is because of flow turning into the flat duct containing the windows enhances mixing. Through the choice of the flow rate, residence times of 0.4−125 s are available.

A 1.07 *m* solution was prepared by dissolving 22.53 g of solid carbohydrazide (Aldrich, 98%) in 250 mL of HPLC grade H_2O which had been sparged with Ar for 30 min to remove dissolved atmospheric gas. The reaction was studied at five temperatures between 503 and 543 K at 275 bar and with flow rates of 2.50−0.02 mL/min, which yield residence times of 0.46−57 s. IR spectra (32 coadded interferograms, 4 cm^{-1} resolution) were collected with a Nicolet 60 SX FTIR spectrometer using 22−25 separate flow rates at each temperature. Each spectrum was ratioed against the spectrum of pure H_2O at the same pressure and temperature to remove as much of the water background absorbance as possible.

The spectra collected supported the existence of a single, liquid phase throughout this study. The relatively constant base line precludes the presence of solids, and $\nu_3(CO_2)$ fails to divide into its P and R branches, which is evidence of the absence of a gaseous phase. However, a small leak existed in the spectroscopy cell during this study which is evident in the appearance of weak rotational fine structure from H_2O vapor

* Corresponding author.
[⊗] Abstract published in *Advance ACS Abstracts,* March 15, 1997.

S1089-5639(96)01806-3 CCC: $14.00

superposed on the desired spectrum. Although this "noise" detracts aesthetically from the spectra, it does not adversely affect the quantitation procedure or subsequent kinetic analysis as it can be accounted for in the curve-fitting procedure. Unfortunately, the cell failed before multiple determinations of the spectra could be made. Our confidence in the data reported here is bolstered by the fact multiple determinations were made for the decarboxylation of malonic acid[8] in a cell of the same design and produced an uncertainty of 35% or less in the rate constants.

Spectral bands were resolved and areas were calculated by using curve-fitting software (Peakfit, Jandel). The absorbances of interest were fitted with a four-parameter Voigt function. The integrated band areas were converted into concentrations (see Results) and plotted against the residence time. The concentration data at residence times of 10 s or less were used for kinetic modeling because plug flow conditions could be assumed.[6] At longer residence times the existence of more laminar-like flow conditions caused broadening into a residence time distribution. The concentration/time data were used to calculate kinetic parameters by optimization of the coupled differential rate equations specified by the various plausible reaction pathways. These equations were solved with a multilevel-single-linkage global optimization routine utilizing a quasi-Newtonian local search method on an IBM RISC6000 Model 530H computer.

Small batch reaction tubes were used to conduct postreaction analysis on several solutions. These 12 cm^3 tubes were constructed from 316 SS and were heated in a fluidized sand bath. Room temperature IR spectra (32 coadded interferograms, 4 cm^{-1} resolution) of the solutions from these reactions were acquired using a liquid cell fitted with ZnSe windows and a 25 mm Ta spacer.

Results

FTIR Spectroscopy of the Reaction. IR spectroscopy of high-temperature solutions of carbohydrazide potentially provide absorbances for the reactants, intermediates, and products. The main problem is that the "fingerprint" region of most of these species is congested and also is partly overlapped by the intense ν_2 absorption of H_2O. Perfect subtraction of the H_2O background is nearly impossible to achieve. Nevertheless, the spectral data provided several kinetic and mechanistic insights.

Spectra of reacting carbohydrazide solutions are illustrated in Figure 1 at several residence times in the flow cell. The behavior of the carbohydrazide reactant is best followed by the absorbance at about 1525 cm^{-1}, which is the amide II (O═C−N−H stretching) mode. A similar absorbance occurs at about 1538 cm^{-1} in a KBr pellet and in an aqueous solution of carbohydrazide at room temperature. The gradual decrease in the energy of this mode from 1538 (295 K) to 1526 (503 K) to 1521 cm^{-1} (543 K) could result from the usual effect of temperature on a molecular vibration or decreasing association of carbohydrazide with the H_2O environment with increasing temperature. Carbohydrazide has an even more intense absorbance at about 1700 cm^{-1} in hot aqueous solution which arises from the C═O stretch, the NH_2 deformation, or the overlap of these two modes. Modes corresponding to these two motions are observed respectively at 1640 and 1685 cm^{-1} in solid carbohydrazide, whereas in aqueous carbohydrazide at room temperature only a medium-intensity absorbance at 1688 cm^{-1} is observed. However, the region between 1620 and 1675 cm^{-1} is obscured by ν_2 of H_2O, making it difficult to determine whether the energies of the NH_2 and C═O vibrations truly occur in the same range in aqueous solution. As with the amide II mode, this absorbance slightly decreased in energy with increasing temperature from 503 to 543 K.

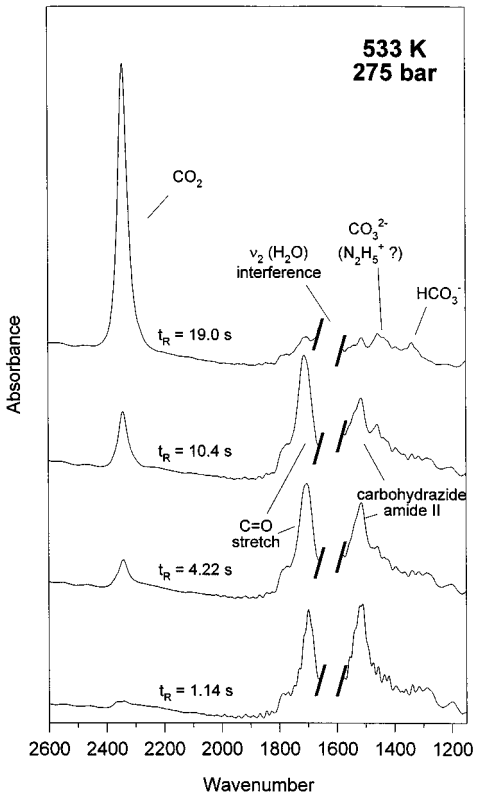

Figure 1. Absorbance IR spectra for hydrothermolysis of 1.07 *m* carbohydrazide at selected residence times in the Pt/Ir diamond flow cell. Assignments are discussed in the text. Longer residence times correspond to greater extent of reaction.

An absorbance for an intermediate species was resolved from the asymmetry of the high-energy side of the absorbance at 1700 cm^{-1}. This absorbance occurs at 1735 cm^{-1} at 503 K and 1723 cm^{-1} at 543 K. A similar absorbance from this species was observed at 1706 cm^{-1} in spectra of solutions at room temperature which were obtained from quenched batch mode experiments. This absorbance might be the amine or amide II mode of the hydrazacarboxylate ion, $NH_2NHC(═O)O^-$, the contact ion pair of its hydrazinium salt, $NH_2NHC(═O)ONH_3$-NH_2, or tetrazolidine (eq 1). We defer discussion of possible intermediates until later in this article.

The only carbon-containing final product observed in the spectrum is CO_2, which is readily identified by its intense ν_3 absorbance at 2344 cm^{-1}. In the spectra during the later stage of the reaction, especially in the lower temperature range, additional absorbances at about 1340 and 1450 cm^{-1} were observed. The lower energy absorbance indicates the presence of HCO_3^- from hydrolysis of some of the CO_2 . The 1450 cm^{-1} absorbance is also present in room temperature spectra of aqueous solutions containing CO_2 and N_2H_4. This absorbance is somewhat higher in energy than ν_3 of aqueous CO_3^{2-} and perhaps arises from the association of $N_2H_5^+$ and CO_3^{2-} in H_2O.

Unassociated nitrogen-containing products (N_2H_4, NH_3) were not spectrally observed. Their IR vibrations have low absorptivity in aqueous solution in the case of N_2H_4 and overlap with H_2O absorbances in the case of NH_3. A weak absorbance at 1140 cm^{-1} is attributable to the N−N stretch of hydrated N_2H_4 in a carbohydrazide solution which was decomposed in a batch reactor and then cooled to room temperature. The absence of additional absorbances suggests that neither significant amounts of other products nor large steady-state concentrations of other intermediates occur during hydrothermolysis of carbohydrazide.

Quantitation of the IR Spectra. The integrated spectral absorbance areas calculated by curve fitting of the spectra are

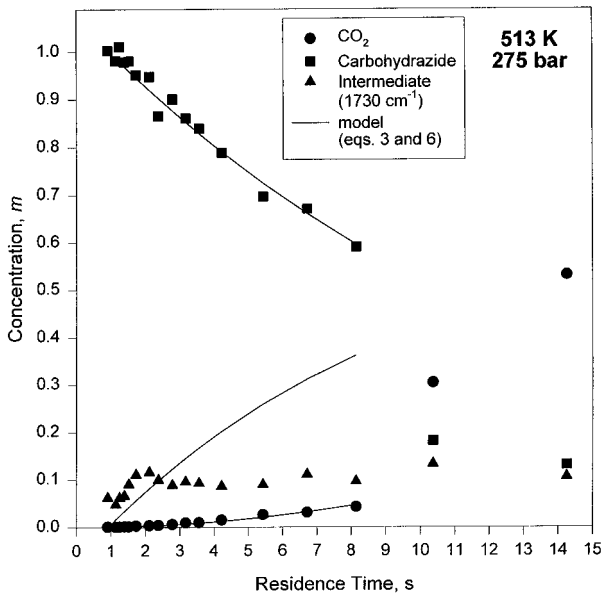

Figure 2. Concentration−time profile of carbohydrazide, CO_2, and the intermediate at 513 K showing that the lumped kinetic scheme (eqs 3 and 6) can describe the reaction up to the initial 10−15% of conversion to CO_2.

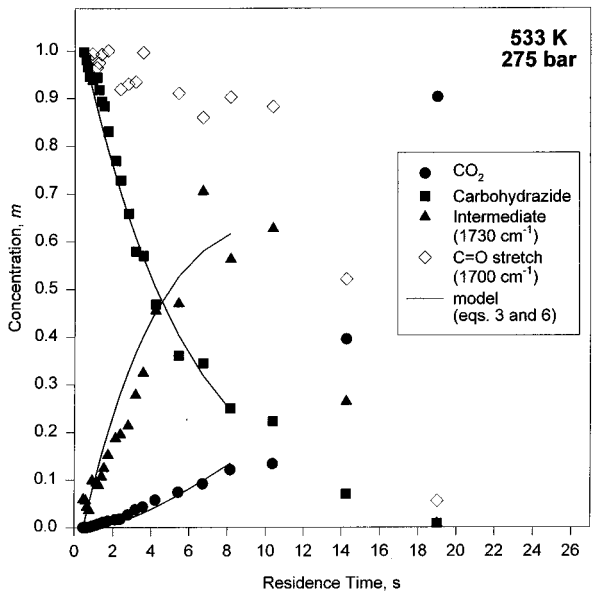

Figure 3. Concentration−time profiles of carbohydrazide, CO_2, the carbonyl vibration, and the apparent intermediate at 533 K. The carbonyl vibration persists, and the intermediate has a relatively constant concentration which suggests that the intermediate is involved in an equilibrium (see text).

the basis for establishing the concentrations of carbohydrazide, the intermediate species, and CO_2 throughout the reaction. The IR absorptivity of aqueous CO_2 has been related previously to its concentration.[7] For other species, the concentrations are approximately linearly related to the area of the characteristic absorbances. In practice, however, establishment of this relation for the various components at each temperature involved finding the best agreement among all of the available information, *i.e.*, consideration of the internal carbon balance, the external calibration data, the density differences, and, where appropriate, equating the maximum reactant or product spectral intensities to the initial concentration of carbohydrazide. The species concentrations thereby obtained were plotted vs the residence time to produce profiles such as are illustrated for two temperatures in Figures 2 and 3.

The carbohydrazide concentration was obtained from the area of the absorbance at 1525 cm^{-1}. In the lower temperature range, initial spectra were available in which no significant reaction had occurred. Thus, the absorbance intensity and concentration could be scaled directly. In the higher temperature sets, some degree of reaction was evident and had to be taken into account even at the shortest residence times. The concentration of CO_2 was calculated directly from the area of the 2344 cm^{-1} absorbance. Spectra taken at longer residence times above 523 K revealed complete conversion to CO_2 on the basis of its constant absorbance intensity and the presence of little or no HCO_3^-. The area of the CO_2 absorbance in these spectra was assigned the same concentration as the initial carbohydrazide concentration and was also independently found to have the correct concentration as predicted by external calibration experiments on aqueous solutions of pure CO_2 at the same temperature and pressure.[7]

The absorbance at about 1700 cm^{-1} for carbohydrazide was more intense than the amide II absorbance. However, it persisted much longer in the spectrum than the amide II absorbance and, therefore, did not follow the carbohydrazide concentration based on the amide II absorbance. In fact, the trend in the intensity of this absorbance was nearly complementary to the absorbance of the CO_2 product (Figure 3). Since this absorbance arises primarily from C═O stretching, its concentration profile could reflect both the reactant and the intermediate species and is an indication that the C═O group survives the initial stage of the reaction.

The concentration trend of the main intermediate appears to be reflected best by the behavior of the 1720−1735 cm^{-1} shoulder of the 1700 cm^{-1} absorbance. Because no external calibration was available for this absorbance, the concentration of this putative intermediate was related to the absorbance intensity by maintaining a constant, running carbon balance between the intermediate, the carbohydrazide reactant, and the CO_2 product. Of course, the concentration of this species is not determined as precisely as those directly measured for carbohydrazide and CO_2. Nevertheless, especially above 523 K, the profiles have the shape logically expected of a single, well-behaved intermediate. Below 523 K, however, Figure 2 reveals somewhat of a plateau in the profile of the intermediate, suggesting the possible existence of an equilibrium involving more than one intermediate species. An unexplained discontinuity in the CO_2 and carbohydrazide concentrations exits in Figure 2 between 8 and 10 s. This discontinuity did not affect the kinetic modeling because concentration data at time greater than 8 s were not used.

Hydrothermal Decomposition Reaction Model and Kinetic Analysis. A global decomposition reaction for carbohydrazide in the hydrothermal environment was given in eq 2. Postreaction analysis of solutions from a batch reactor confirms that hydrazine is the main nitrogen-containing product. However, at high temperature a small amount of NH_3 was detected, primarily by its odor, and probably originates from decomposition of aqueous N_2H_4, which is known to occur at elevated temperature and pressure.[9]

The spectroscopic data in Figure 1 and the concentration profiles in Figures 2 and 3 reveal additional features about eq 2 which help to define the hydrothermolysis pathway. First, the initial step of the reaction, as reflected by the concentration profile of carbohydrazide, has effective first-order (or pseudo-first-order) rate behavior according to Figure 4. Second, the spectroscopic data reveal that the decomposition of carbohydrazide to CO_2 proceeds through at least one intermediate. The exact nature of the intermediate(s) is uncertain; however, the identity is not essential to construction of a kinetic model. Third,

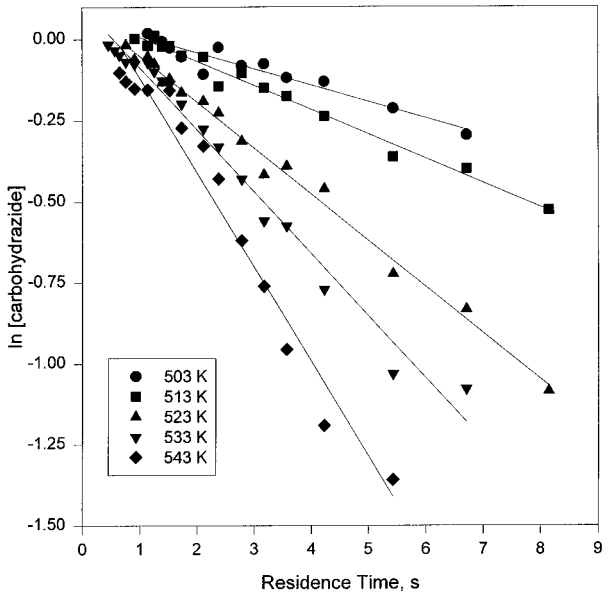

Figure 4. Effective first-order rate plots for the decomposition of the carbohydrazide reactant. The nonzero intercept originates from assumptions about the cell volume and the concentration calibration where only a small change occurs.

the existence of a second intermediate occurring between the first intermediate and formation of CO_2 might be responsible for the small deficiency (<8%) in the carbon balance of the concentration profiles just prior to and through the early stage of the rapid rise in concentration of CO_2. If an additional intermediate does exist, then its steady-state concentration is low or its IR absorptivity is small because no clear spectral evidence exists for it. Fourth, the initial 10−15% of the last stage of the reaction, which involves the production of CO_2, occurs relatively slowly according to Figures 2 and 3. At greater percentage conversion, the rate of formation of CO_2 increases rapidly, which suggests that autocatalysis takes place. Since the rate of decay of carbohydrazide reactant retains effective first-order behavior throughout the reaction, the catalyzed step must occur after the initial reaction of carbohydrazide.

The spectrally derived reaction details outlined above are captured by the kinetic model in eqs 3−5.

$$(NH_2NH)_2C{=}O \xrightarrow[\text{slow}]{k_1} \text{intermediate 1} \qquad (3)$$

$$\text{intermediate 1} \xrightarrow[\text{slow}]{k_2} \text{intermediate 2} \qquad (4)$$

$$\text{intermediate 2} \xrightarrow[\text{fast}]{k_3} CO_2 + 2N_2H_4 \qquad (5)$$

Optimization of the fit of the concentration−time data with the set of differential rate equations constructed for eqs 3−5 was extensively explored, including the use of different reaction orders for eqs 4 and 5, incorporation of reversibility into eqs 3−5, and inclusion of autocatalysis in eqs 4 and 5. All of these models either failed to converge or fit the experimental data poorly.

In place of eqs 3−5, a lumped kinetic scheme incorporating two rate parameters described by eqs 3 and 6 was used.

$$\text{intermediate} \xrightarrow{k'_2} CO_2 + 2N_2H_4 \qquad (6)$$

In this model, k'_2 is recognizable as the composite of the rate constants for eqs 4 and 5; however, since the velocity of eq 5 is expected to be much larger than that of eq 4, the value of k'_2 primarily reflects k_2 in eq 4. In effect, without concentration data for "intermediate 2", the three-parameter model of eqs 3−5 is underspecified and yields unsatisfactory results. The lumped kinetic scheme cannot account for the autocatalytic behavior observed after 10−15% of the CO_2 is formed. Therefore, the model was only used to fit the concentrations up to 10% conversion to CO_2. The interference of the apparent equilibrium involving the intermediate at 503 and 513 K produced questionable results when the intermediate (~1730 cm^{-1} absorbance) concentration data were included in the optimization of eqs 3 and 6. Consequently, only the $(NH_2NH)_2C{=}O$ and CO_2 data were used in the final modeling. The concentration of the intermediate predicted by the model closely resembles the experimental data above 513 K (Figure 3). The resulting first-order rate parameters are listed in Table 1, and the Arrhenius plots and parameters are shown in Figure 5. It is interesting to note that k_1 is larger than k'_2 when $T > 446$ K. This is the isokinetic temperature below which this rate relation is reversed. The Arrhenius parameters for k_1 are essentially the same as those for hydrothermolysis of urea,[6,7] which could imply a key role for H_2O in the transition state of decomposition of both compounds. The overall mechanism of decomposition need not necessarily be the same.

TABLE 1: Rate Constants for the Hydrothermolysis Steps of 1.07 *m* Carbohydrazide at 275 bar

temp, K	k_1,[a] s^{-1}	k_1,[b] s^{-1}	k'_2,[b] s^{-1}
503	0.051 ± 0.004	0.056 ± 0.016	0.019 ± 0.017
513	0.075 ± 0.003	0.072 ± 0.013	0.031 ± 0.022
523	0.142 ± 0.003	0.13 ± 0.04	0.036 ± 0.043
533	0.192 ± 0.007	0.18 ± 0.06	0.043 ± 0.056
543	0.241 ± 0.016	0.25 ± 0.11	0.057 ± 0.126

[a] Slopes from Figure 4. [b] Kinetic model.

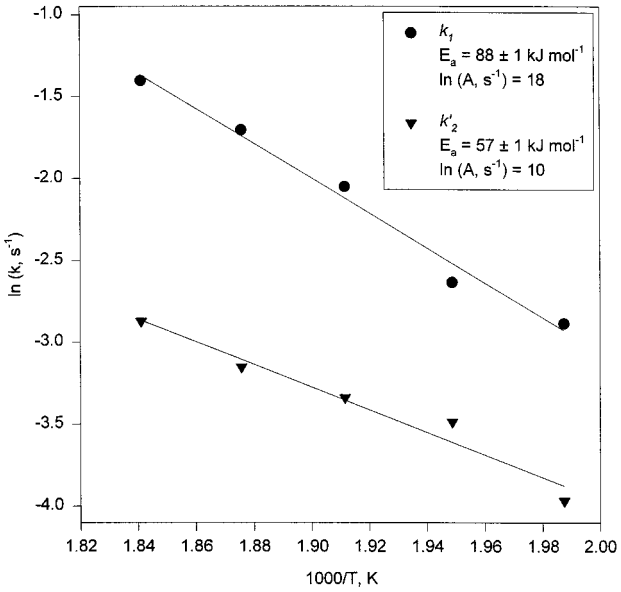

Figure 5. Arrhenius plots and the resulting parameters for eqs 3 and 6 in the kinetic analysis of the hydrothermal conversion of carbohydrazide to the final products.

Discussion

Several features of the mechanism of hydrothermolysis of carbohydrazide are revealed by these direct spectral studies during the reaction. The rate constant k_1 and the resulting Arrhenius parameters for this step represent an effective first-order or pseudo-first-order process. The rate constant k'_2, on the other hand, is the net rate of the remaining steps leading to

formation of CO_2. Therefore, discussion of the molecular interpretation is appropriate for k_1, but not for k'_2.

Clearly, the identity of the intermediate species is a central issue in the mechanism. Two types of potential intermediates were mentioned in the Introduction based on pyrolysis and hydrolysis reactions. During pyrolysis, cyclization−elimination leads to a tetrazolidine and N_2H_4 (eq 1). We also imagined intermediates that could result from C−N bond cleavage leading to aminoisocyanate,[10] H_2NNCO, and diazenecarboxaldehyde,[11,12] HN═NC(═O)H. Neither of these compounds has sufficient thermal stability to survive under the conditions of this work. Moreover, the isocyanate absorbance is expected to be intense and was not detected.

The possibility that the tetrazolidine product of eq 1 or its isomer *p*-urazine, $OC(NHNH)_2CO$, are intermediates was more thoroughly explored. The presence of *p*-urazine is unlikely because it is known to be thermally unstable with respect to rearrangement to the tetrazolidine.[13] IR spectra of aqueous solutions of the latter compound at room temperature contain an absorbance at 1710 cm^{-1}, which is similar in energy to the absorbance of the intermediate at similar conditions (1706 cm^{-1}). However, this absorbance arises from the C═O stretch of the tetrazolidine which is higher in energy than the similar mode of carbohydrazide and the intermediate (1688 cm^{-1}). Therefore, it is not likely that the tetrazolidine is responsible for the 1730 cm^{-1} absorbance observed at high temperature. Moreover, batch mode experiments indicated that tetrazolidine in H_2O gave the same final products as carbohydrazide but that the rate of conversion is at least an order of magnitude slower. Furthermore, the apparent first-order decay of the concentration of carbohydrazide shown in Figure 4 conflicts with eq 1 in which the decay of the carbohydrazide should have simple second-order kinetics. The conclusion is that the tetrazolidine is not the main intermediate under hydrothermolysis conditions. It would be more probable instead that hydrothermolysis of the tetrazolidine occurs to produce CO_2 and carbohydrazide rather than the carbohydrazide producing the tetrazolidine.

The kinetics and spectroscopy provide evidence that insertion of H_2O produces the reaction intermediate(s). The decay of carbohydrazide was indicated by the disappearance of the amide II vibration resulting from the disruption of the −NH−C(═O)− unit. The concentration profile establishes that the decay is effectively a first-order or a pseudo-first-order process. On the other hand, the spectra also revealed that the C═O group is preserved in the intermediate species due to the persistence of the absorbance at about 1700 cm^{-1}. Since N_2H_4 and CO_2 are the only products of the overall pathway, it is reasonable to assume that this first step involves the cleavage of one of the C−N bonds. This pseudo-first-order initial step can be achieved by hydrogen bonding of an H atom of H_2O and the lone pair of electrons on an α-N atom, followed by nucleophilic attack of H_2O on the carbon atom (eq 7). The salt-like product is stable in H_2O at room temperature.[14]

$$(NH_2NH)_2C{=}O + H_2O \rightarrow NH_2NHC(=O)O^{(-)}\cdot^{(+)}N_2H_5 \quad (7)$$

Consistent with this reaction is the fact that the *A* factor derived for k_1 (Figure 5) produces $\Delta S^{\ddagger} = -108$ J mol^{-1} K^{-1} at 523 K. A large negative value of $\Delta S^{\ddagger}$ is expected when a solvent molecule is consumed in the reaction.[15] The resulting salt-like product could exist as solvent-separated ions or as the contact ion pair. The insensitivity of the C═O stretching vibration to temperature-induced changes in the environment suggests that charge is somewhat delocalized, which is favored for the contact ion pair. In reality it is reasonable that equilibria (eqs 8 and 9) exist in the hydrothermal regime

$$NH_2NHC(=O)O^- + N_2H_5{+} \rightleftarrows NH_2NHC(=O)O^{(-)}\cdot^{(+)}N_2H_5 \quad (8)$$

$$NH_2NHC(=O)O^{(-)}\cdot^{(+)}N_2H_5 \rightleftarrows NH_2NHC(=O)OH + N_2H_4 \quad (9)$$

but the competing effects of the smaller bulk dielectric constant of H_2O[16] and larger value of K_w[17] at the temperatures used here make it difficult to discuss the details. A shift in eq 8 to the left-hand side could explain why a plateau exists in the concentration of the intermediate in the lower temperature range of study (Figure 2).

The hydrazacarboxylic acid component in eq 9 is known to equilibrate with CO_2 and N_2H_4 in aqueous solution at room temperature (eq 10).[5] The rate constant k'_2 is a global representation of eqs 8−10.

$$NH_2NHC(=O)OH \rightleftarrows CO_2 + N_2H_4 \quad (10)$$

The apparent autocatalytic increase in rate of the production of CO_2, which occurs after 10−15% of the CO_2 is formed, could result from the effect that CO_2 has on $[H^+]$ as the reaction proceeds. Because CO_2 is a weak acid anhydride, the formation of HCO_3^-, which is detected in the end stage of the reaction (Figure 1) raises $[H^+]$. Hence, N_2H_4 is converted to $N_2H_5^+$, which is a reactant in eqs 8 and 9. The net effect is that k'_2 becomes larger as CO_2 is produced.

In conclusion, *in situ* IR spectroscopy during the hydrothermolysis of carbohydrazide enables details of the reactions to be learned. In particular, the number of potentially possible intermediates can be reduced to a relatively narrow class based on consistency with the spectra and chemistry. The rates of individual steps, as opposed to only the overall process, are obtained. The existence of autocatalysis is detected. It could be argued from a practical point of view that the only essential chemical knowledge needed about hydrothermolysis of carbohydrazide as an antioxidant is the fact that N_2H_4 is produced. On the other hand, the safety and practice in new directions and uses of hydrothermal chemistry, such as in waste destruction and organic synthesis, may require more fundamental insight about the various reaction pathways. Direct spectral studies provide this opportunity.

Acknowledgment. We are grateful to the Army Research Office for support of this work through Grant DAAL03-92-G-0174.

References and Notes

(1) Bossler, J. F.; Hamann, H. C.; Kinstler, W. I. US Patent, 5,108,624, March 12, 1990 (CA 117:137352v).
(2) Akol'zin, A. P.; Klochkova, B. V. G.; Balsbanov, A. E. *Tepioenergetika (Moscow)* **1988**, 61−63 (CA 109:196843p).
(3) Van de Wissel, J. T. M. *Polytech. Tijdschr. Proscestech.* **1991**, *46*, 40−44.
(4) Nachbaur, E.; Baumgartner, E.; Schober, J. *Proc. Eur. Symp. Therm. Anal.* **1981**, 417−421.
(5) Ravindranathan, O.; Patil, K. C. *Proc. Indian Acad. Sci. (Chem. Sci.)* **1985**, *95*, 345−356.
(6) Schoppelrei, J. W.; Kieke, M. L.; Wang, X.; Klein, M. T.; Brill, T. B. *J. Phys. Chem.* **1996**, *100*, 14352.
(7) Kieke, M. L.; Schoppelrei, J. W.; Brill, T. B. *J. Phys. Chem.* **1996**, *100*, 7455−7462.
(8) Maiella, P. J.; Brill, T. B. *J. Phys. Chem.* **1996**, *100*, 14352.
(9) Masten, D. A.; Foy, B. R.; Harradine, D. M.; Dyer, R. B. *J. Phys. Chem.* **1993**, *97*, 8557−8559.
(10) Teles, J. H.; Maier, G. *Chem. Ber.* **1989**, *122*, 745−748.
(11) Colquhoun, H. M.; Henrick, K. *Inorg. Chem.* **1981**, *20*, 4074−4078.

(12) Howell, J. M.; Kirschenbaum, L. J. *J. Am. Chem. Soc.* **1976**, *98*, 877−885.
(13) Neugebauer, A.; Fischer, H. *Liebigs Ann. Chem.* **1982**, 387−395.
(14) Stolle, R.; Hofmann, K. *Chem. Ber.* **1904**, *37*, 4523−4525.
(15) Connors, K. A. *Chemical Kinetics*; VCH: New York, 1990; p 220.
(16) Uematsu, M.; Franck, E. U. *J. Phys. Chem. Ref. Data* **1980**, *9*, 1291−1306.
(17) Marshall, W. L.; Franck, E. U. *J. Phys. Chem. Ref. Data* **1981**, *10*, 295−304.